ACS APPLIED MATERIALS & INTERFACES

Research Article

www.acsami.org

Single-Molecule Resolution of Protein Dynamics on Polymeric Membrane Surfaces: The Roles of Spatial and Population Heterogeneity

Blake B. Langdon,[†] Roya B. Mirhossaini,[†] Joshua N. Mabry,[†] Indira Sriram,[†] Ajay Lajmi,[‡] Yanxia Zhang,[§] Orlando J. Rojas,[§,∥] and Daniel K. Schwartz*,[†]

[†]Department of Chemical and Biological Engineering, University of Colorado Boulder, Boulder, Colorado 80309, United States

[‡]Pall Life Sciences, 8780 Ely Road, Pensacola, Florida 32514, United States

[§]Departments of Forest Biomaterials and Chemical and Biomolecular Engineering, North Carolina State University, Raleigh, North Carolina 27695, United States

[∥]School of Chemical Technology, Aalto University, 00076 Aalto, Finland

Supporting Information

ABSTRACT: Although polymeric membranes are widely used in the purification of protein pharmaceuticals, interactions between biomolecules and membrane surfaces can lead to reduced membrane performance and damage to the product. In this study, single-molecule fluorescence microscopy provided direct observation of bovine serum albumin (BSA) and human monoclonal antibody (IgG) dynamics at the interface between aqueous buffer and polymeric membrane materials including regenerated cellulose and unmodified poly(ether sulfone) (PES) blended with either polyvinylpyrrolidone (PVP), polyvinyl acetate-*co*-polyvinylpyrrolidone (PVAc-PVP), or polyethylene glycol methacrylate (PEGM) before casting. These polymer surfaces were compared with model surfaces composed of hydrophilic bare fused silica and hydrophobic trimethylsilane-coated fused silica. At extremely dilute protein concentrations (10^{-5}–10^{-7} mg/mL), protein surface exchange was highly dynamic with protein monomers desorbing from the surface within ~1 s after adsorption. Protein oligomers (e.g., nonspecific dimers, trimers, or larger aggregates), although less common, remained on the surface for 5 times longer than monomers. Using newly developed super-resolution methods, we could localize adsorption sites with ~50 nm resolution and quantify the spatial heterogeneity of the various surfaces. On a small anomalous subset of the adsorption sites, proteins adsorbed preferentially and tended to reside for significantly longer times (i.e., on "strong" sites). Proteins resided for shorter times overall on surfaces that were more homogeneous and exhibited fewer strong sites (e.g., PVAc-PVP/PES). We propose that strong surface sites may nucleate protein aggregation, initiated preferentially by protein oligomers, and accelerate ultrafiltration membrane fouling. At high protein concentrations (0.3–1.0 mg/mL), fewer strong adsorption sites were observed, and surface residence times were reduced. This suggests that at high concentrations, adsorbed proteins block strong sites from further protein adsorption. Importantly, this demonstrates that strong binding sites can be modified by changing solution conditions. Membrane surfaces are intrinsically heterogeneous; by employing single-molecule techniques, we have provided a new framework for understanding protein interactions with such surfaces.

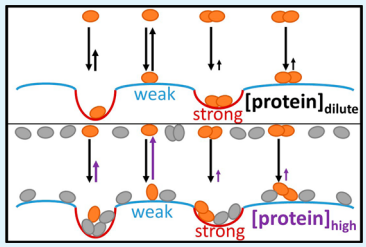

KEYWORDS: *protein adsorption, ultrafiltration, membrane fouling, single-molecule, total internal reflection fluorescence microscopy (TIRFM)*

INTRODUCTION

Membrane processes are increasingly used in the commercial purification and sterilization of protein biopharmaceuticals.[1−4] However, membrane fouling, due to pore narrowing, pore plugging, and cake formation, is a fundamental challenge to be addressed when implementing and optimizing membrane separation.[5] Membrane fouling ultimately reduces separation efficiency and may contribute to protein aggregates or other impurities in downstream products.[6,7]

Although protein fouling of membranes has been widely studied, the molecular-level mechanisms, including protein adsorption, aggregation, and unfolding, remain poorly understood. For example, online process measurements often provide macroscopic information (e.g., flux and transmembrane pressure drop), measuring the effects of protein adsorption only indirectly.[8] By varying the feed concentration and other process parameters, models of fouling mechanisms have been proposed and evaluated.[9,10] For example, Kelly et al. showed that microfiltration membrane flux declined more rapidly when bovine serum albumin (BSA) protein oligomers (e.g., dimers, trimers) and aggregates were present (unfiltered solutions) in the feed solution than when only BSA monomers were present

Received: November 6, 2014
Accepted: January 22, 2015
Published: January 22, 2015

DOI: 10.1021/am507730k
ACS Appl. Mater. Interfaces 2015, 7, 3607−3617

(300 kDa filtered solutions). Further, they observed that membrane flux continued to decline in sequential filtrations of unfiltered and filtered BSA solutions. On the basis of these findings, they proposed a two-step process in which BSA aggregates deposited quickly on pore walls, narrowing or blocking the flow, and subsequently served as nucleation sites for BSA aggregation, further reducing membrane flux.[11,12] More detailed information about protein membrane fouling has been obtained by other surface sensitive techniques such as quartz crystal microbalance (amount of protein),[13,14] atomic force microscopy (AFM) (protein layer topography),[15] and attenuated total reflectance/Fourier transform infrared spectroscopy (ATR/FTIR) (protein conformation).[16] However, these techniques measure ensemble-averaged or net behavior, and are generally insensitive to the various forms of heterogeneity and complexity that characterize these processes.

Single-molecule total internal reflection fluorescence microscopy (sm-TIRFM) is uniquely suited to separate competing kinetic protein processes (e.g., adsorption, desorption, and interfacial diffusion) as well as to capture the entire distribution of protein dynamics.[17,18] In previous work at oil−water and solid−water interfaces, protein surface species (e.g., monomers, dimers, trimers, larger oligomers, and larger aggregates) were found to exhibit distinct behaviors.[19,20] For example, protein oligomers were found to reside on solid surfaces longer and execute smaller and fewer diffusive steps than protein monomers.[19] Surface spatial heterogeneity (e.g., hydrophobic and hydrophilic regions, surface defects) has also been identified by examining the spatial variation of interfacial molecular dynamic.[21,22] In the work reported here, we used single-molecule tracking capabilities to characterize heterogeneity involving protein populations and surface chemistry and topographic variation on polymer thin films relevant to ultrafiltration.

Many factors can determine the mechanism and rate of membrane fouling, including flow hydrodynamics and protein and membrane physicochemical properties. In this work, we have focused on the latter by comparing the interactions of two different proteins, bovine serum albumin (BSA) and a monoclonal antibody (IgG), on several polymer films under no-flow conditions. The distinct differences in the molecular shape, size, and isoelectric point of BSA and IgG, both commonly used protein classes in the separations literature, allowed us to begin to assess the relative universality of protein interactions with these surfaces. For example, BSA and IgG have opposite net charges at a pH of 7.4, the molecular weight of IgG is 2 times as large as that of BSA, and the secondary structure of BSA is dominated by α helices whereas IgG is mainly composed of β sheets (see the Materials and Methods section).[23] Therefore, BSA and IgG might be expected to be attracted to surfaces of opposite charges as well as bind, diffuse, or unfold differently on various surfaces.

Regenerated cellulose (RC) and unmodified poly(ether sulfone) (PES) were used in our experiments because they are commonly used membrane materials.[16,24] Because PES is hydrophobic, polymeric "wetting agents" are often either blended with PES prior to casting or post-treated after casting to produce more hydrophilic membrane materials.[25] In our experiments, we blended PES with either polyvinylpyrrolidone (PVP), poly(vinyl acetate)-*co*-polyvinylpyrrolidone (PVAc-PVP), or poly(ethylene glycol) methacrylate (PEGM) prior to casting. All prepared polymer surfaces (RC and PES blends) showed similar hydrophobicity, thickness, and roughness (see the Materials and Methods section and the Supporting Information) and were expected to be negatively charged at neutral pH in 158 mM phosphate buffered saline.[26,27] These surfaces were also compared to model hydrophilic, negatively charged fused silica (FS) and hydrophobic trimethylsilane-modified (TMS) surfaces. All of the surfaces differed in their composition, hydrogen-bonding capacity, and, as we explore below, their spatial heterogeneity.

We investigated interfacial protein dynamics at (1) extremely dilute ($\sim 10^{-7}$ mg/mL) and (2) higher (0.3−1.0 mg/mL) protein concentration conditions, which are relevant to early and intermediate processes, respectively, in membrane fouling. Although these protein concentrations were lower than may be used in industrial ultrafiltration (e.g., 100−200 mg/mL IgG),[1] they were useful in contrasting protein−surface interaction in the absence and presence of protein−protein interactions. For the higher concentration experiments, the same protein concentration was used across all surfaces studied, as is typical in macroscopic membrane fouling studies.[15,16] While less common, both protein oligomers and anomalously strong adsorption sites accounted disproportionately for longer-lived surface species that may nucleate further protein surface accumulation. We found that these effects were modulated by surface chemistry and protein concentration.

MATERIALS AND METHODS

Thin Polymer Film Preparation and Characterization. *Cleaning and Preparation of Surfaces.* All surfaces were prepared using fused silica (FS) and silicon wafers (Mark Optics). Wafers were cleaned by immersion in a warm piranha solution (concentrated sulfuric acid (Fisher Scientific) and 30% aqueous hydrogen peroxide (Fisher Scientific), 3:1 v/v) for 1 h then treated with UV-ozone for 1 h, as described previously.[19] ***Caution***: piranha solution is aggressive and explosive. Never mix piranha waste with solvents. Check the safety precautions before using it. Trimethylsilane (TMS) coatings were prepared by exposing wafers to hexamethyldisilazane (Fisher Scientific) vapor for 18 h at room temperature. FS and TMS served as model surfaces, representing very hydrophilic and very hydrophobic surfaces, respectively. A methyl-polyethylene glycol silane (mPEG-silane; Gelest) self-assembled monolayer was formed via solution deposition as previously reported[19] and used as an anchoring layer for PEGM/PES polymer thin films. TMS was used as an anchoring layer for all other polymer thin films.

Polymer films were prepared by spin-coating a polymer solution in organic solvent (i.e., toluene, dichloromethane, or *N*,*N*-dimethylformamide) onto a wafer. A regenerated cellulose precursor trimethylsilyl cellulose (TMSC) was prepared as previously reported.[28] PES (molecular weight (MW) 48 000 Da), PVP (MW 1,300 000 Da), and PVAc-PVP (MW 47 000 Da) were used for PVP/PES and PVAc-PVP/PES films. PEG monomethacrylate (MW 400 Da) and PEG dimethacrylate (MW 400 Da) were polymerized with PES (MW 48 000 Da) to form PEGM/PES films. Molecular structures of the polymeric materials used are shown in Figure S1 and additional polymer film preparation details are provided in the Supporting Information.

Contact-Angle Measurements. A custom-built contact-angle goniometer was used to measure the static water contact angle (WCA) on the surface of the materials considered in these studies. WCAs were measured by depositing a 1 μL drop of deionized water, purified to 18.2 MΩ cm (Millipore Mill-Q UV+), on the surface. A minimum of five drops on each of at least two independent samples were averaged and reported in Table 1. Interestingly, all membrane polymer films had similar WCAs and, therefore, similar hydrophobicities and macroscopic surface energy. Nearly complete wetting was observed on bare FS, consistent with previous work. The WCA measured on TMS was 95 ± 3°, also consistent with previously measured values.[19] Prior to hydrolysis, the TMSC film WCA was 94 ±

DOI: 10.1021/am507730k
ACS Appl. Mater. Interfaces 2015, 7, 3607−3617

Table 1. Polymer Thin Film Characteristics[a]

polymer film	static WCA (deg)	thickness (nm)	RMS roughness (nm^2)
PVP/PES	60 ± 3	26 ± 7	0.47 ± 0.07
PVAc-PVP/PES	54 ± 1	24 ± 1	0.98 ± 0.04
PEGM/PES	50 ± 1	30.6 ± 0.4	0.18 ± 0.09
RC	51 ± 11	23.5 ± 0.9	1.2 ± 0.1

[a]The standard deviation between at least three measurements is reported (see the Contact-Angle Measurements, Ellipsometry, and Atomic Force Microscopy sections for details).

3°. This was similar to previously reported values for thin films prepared via Langmuir–Blodgett deposition (85° and 100° for static and advancing WCA).[29,30] After hydrolysis, RC had a static WCA of 51 ± 11°, consistent with previous cellulose films prepared using this approach.[29−31]

Ellipsometry and FTIR Spectroscopy. Both ellipsometry and FTIR spectroscopy were performed on films deposited on silicon substrates (WRS Materials). Polymer film thicknesses were measured in air with a variable angle spectroscopic ellipsometer (V-VASE, J.A. Woollam). For each surface, a minimum of three separately prepared surfaces were measured and account for the error in each thickness value. Changes in amplitude, Ψ, and phase, Δ, were measured at 5° intervals for 60° to 80° and over the spectroscopic range of 400–900 nm. An isotropic, three-interface optical model (composed of air, polymer film, silicon dioxide, and silicon) was used to determine the polymer film layer thickness. TMSC surfaces had a thickness of 60.5 ± 0.2 nm, which was reduced to 23.5 ± 0.9 nm when hydrolyzed to RC. Hydrolysis was confirmed with Fourier Transform Infrared Spectroscopy (FTIR) using a Thermo Scientific Nicolet 6700 FT-IR in a specular reflection geometry. The TMSC IR spectrum showed typical wavenumber ν(Si–C) signals near 1243, 878, 839, and 752 cm^{-1} and no hydroxyl signal.[32] When hydrolyzed, the RC IR spectrum had no measurable ν(Si–C) signals and had a strong, broad ν(O–H) signal between 3450 and 3400 cm^{-1}, suggesting that the hydrolysis of trimethyl silane groups was essentially complete (see Figure S2 in the Supporting Information).

Atomic Force Microscopy (AFM). A Nanoscope III instrument (Digital Instruments, now Bruker) using tapping mode in air was used to image the polymer films. Reported roughness values were averaged from 1 × 1 μm areas on at least three samples. Representative AFM images of all polymer films are shown in Figure S3 in the Supporting Information.

Protein Labeling and Solution Preparation. Alexa Fluor 555 labeled BSA (MW 67 000 Da, isoelectric point (pI) 4.7)[33] was purchased from Invitrogen (5 dyes per protein molecule on average). A purified humanized IgG1 monoclonal antibody (MW ∼ 146 000 Da, calculated pI ∼ 8.9), here denoted as "IgG", was used in these studies. IgG was fluorescently labeled with Alexa Fluor 555 dye using a commercially available protein labeling kit (Invitrogen); the primary amine dye conjugation chemistry was performed in phosphate buffered saline at pH ∼8.3. The fluorescently labeled proteins were separated from unreacted free dyes using a Bio-Scale mini Bio-Gel $P\overline{6}$ desalting cartridge (Bio-Rad) on a BioLogic DuoFlow medium-pressure chromatography system with UV–visible detection (Bio-Rad), which showed visual separation between low molecular weight unreacted dye and high molecular weight fluorescently labeled IgG. IgG was labeled on average with 8 dyes per protein molecule determined with a UV–visible spectrophotometer (Thermo Scientific).

All experiments were performed in phosphate buffered saline (Gibco, pH 7.4). Extremely dilute protein concentration experiments were performed with labeled protein concentrations of 10^{-5}–10^{-6} and 10^{-3}–10^{-7} mg/mL for IgG and BSA, respectively, such that single molecules could be resolved as distinct diffraction limited spots and protein surface coverage were similar (see the Supporting Information, Table S3). For high concentration experiments, solutions contained unlabeled proteins at 0.3 or 1.0 mg/mL concentrations of IgG or BSA, respectively, and labeled protein in the same concentrations that were used for dilute concentration experiments on the given functionalized surface.

Image Acquisition and Single-Molecule Tracking. Fluorescently labeled proteins were imaged with a custom-built prism-based TIRFM system and flow cell as previously described,[19] and were illuminated by a 532 nm DPSS LASER (Cobalt Samba) at a power density of 6 ± 1 $\mu W/\mu m^2$. For each experiment, multiple movies (i.e., sequences of 1000 images) were captured with an acquisition time of 200 ms. This acquisition time provided a satisfactory signal-to-noise ratio while also allowing us to capture protein surface dynamics. The flow cell was maintained at 25 ± 1 °C, and flow was stopped prior to movie capture in order to increase the stability of our optical setup. Additionally, no significant differences in adsorption rates were observed over the course of a 2 h experiment. For each type of surface (FS, TMS, or polymer film), protein dynamics were captured on at least three independent surface areas.

Single-molecule trajectories were constructed by identifying objects in each frame and then linking objects from frame-to-frame, as described previously.[17,19] Briefly, diffraction-limited objects in each frame were identified by convoluting the image with a disk matrix, subtracting local background, and thresholding the image (i.e., groups of pixels above the threshold were identified as objects). An object's intensity in each frame was the total intensity of all contiguous pixels after subtraction of the local background intensity. Object positions were calculated as the centroid of intensity with a localization precision of ∼50 nm.[22] Molecular trajectories were constructed by linking an object's center of intensity to the nearest center of intensity within a distance (i.e., tracking radius) of 4 pixels (1.08 μm) in subsequent frames. Protein kinetics were found to be insensitive to the tracking radius selected (see Figure S12 in the Supporting Information). Surface residence times were calculated as the number of consecutive frames for which an object was identified, multiplied by the acquisition time.

Data Analysis. *Single-Molecule Trajectory Analysis.* Accumulated surface residence times were used to calculate the complementary cumulative residence time distribution (CRTD), which represents the fraction of molecules that remain on the surface for time t or longer after the initial adsorption event. CRTDs have the advantage of being especially sensitive to rare populations compared to raw distributions.[34] Assuming that the surface residence time of a given protein population follows first-order desorption kinetics, the CRTD for the sum of all populations can be described using an exponential mixture model

$$p(t) = \sum_i f_i e^{-t/\tau_i} \quad (1)$$

where $p(t)$ is the probability that a given object will have a residence time of t or greater. Each population is denoted with a subscript i and is described by the fraction of molecules, f_i, belonging to the population and a characteristic residence time, τ_i (i.e., the inverse of the first-order desorption rate constant). The mean surface residence time, τ, can be calculated as $\tau = \sum_i^p f_i\tau_i$, where p is the total number of populations. Further details of constructing CRTDs and additional calculations have been described previously.[19,34] Trajectories spanning two or more images were used to construct experimental CRTDs due to the sensitivity of single image object identification to noise. For each experiment, a CRTD was constructed for each movie and fit using eq 1. These fit values were averaged by weighting each movie by the number of objects observed in that movie; the error reported corresponds to the standard error of the weighted fit values.

In previous work, using fibrinogen proteins, we identified a correlation between residence times and fluorescence intensity, where molecules with a higher mean fluorescence intensity, (determined to represent preformed oligomers), resided on the surface for longer time intervals.[19] In this work, we used fluorescence intensity to separate protein monomers from oligomers. A representative histogram of the mean of the fluorescence intensities of all frames comprising each observed trajectory is shown in Figure 1b. An object's fluorescence intensity for each frame was calculated as above, the total intensity of all contiguous pixels after subtracting a

DOI: 10.1021/am507730k
ACS Appl. Mater. Interfaces 2015, 7, 3607–3617

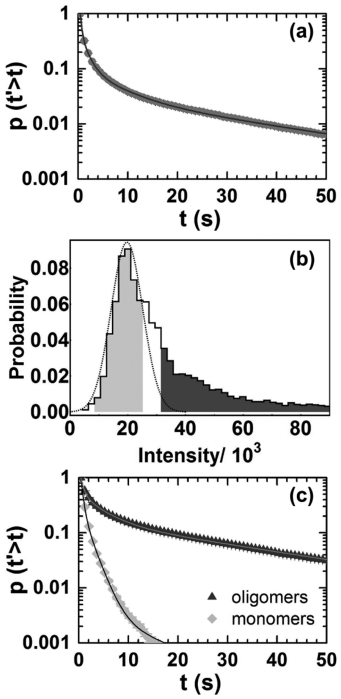

Figure 1. (a) CRTD for IgG on RC at an extremely dilute protein concentration. (b) Probability distribution of the mean fluorescence intensities of IgG molecule trajectories on RC. The fluorescence intensities of objects identified as monomers and oligomers are highlighted in light and dark gray, respectively. (c) CRTDs for IgG monomers and oligomers on RC as identified by their mean fluorescence intensities. Equation 1 population fit parameters are tabulated in Table S1 in the Supporting Information.

local background intensity. Because monomers were the dominant species in solution, we expected the lowest and dominant intensity peak to describe the monomeric species. This peak was successfully approximated as a normal distribution. Only the left-hand side of the lowest intensity peak was fit to a Gaussian distribution, since the right-hand side overlapped significantly with higher intensity peaks. Molecular trajectories with mean intensities within the lower 95% and the upper 68% confidence intervals were considered monomers while molecular trajectories above the monomer normal distribution mean by 3 standard deviations (2–3 times the monomer peak mean for all protein–surface combinations) were considered oligomers (consisting of dimers, trimers, and potentially larger oligomers). Such consistent and conservative intervals were selected in order to ensure that only monomer or only oligomer dynamics were examined for each protein–surface combination. We could then characterize interfacial dynamics (e.g., surface residence time) of monomers and oligomers separately by selecting molecular trajectories by their mean fluorescence intensity.

Super-Resolution Imaging and Adsorption Site Analysis. A variation of the localization technique known as "motion blur" point accumulation for imaging in nanoscale topography (mbPAINT)[35] was used to construct super-resolution maps of protein adsorption events and adsorption sites. This technique takes advantage of increased localization precision from taking the centroid of the point spread function (~50 nm, compared to a camera pixel of 227 nm). By creating these maps, we were able to accurately measure adsorption and desorption kinetics for molecular-scale surface sites and, importantly, identify distinct populations of sites. The specific mapping methods were described previously by Mabry et al.[22] The initial position of each molecular trajectory was placed on a pseudoimage with 22.7 nm pixels (10× smaller than camera pixels) and blurred such that an adsorption center was represented by Gaussian peak with a standard deviation σ_{loc} and an amplitude of 1 adsorption event. Super-resolution adsorption event maps were constructed by summing all blurred pseudoimage adsorption events. On these adsorption event maps, adsorption sites were identified as any group of connected pixels with an amplitude of ≥1 adsorption event.

The adsorption event count, n, of a given site was defined by the maximum pixel value of all pixels assigned to that site. A probability histogram of adsorption events on a surface's adsorption sites was constructed and could be described by a Poisson mixture model, $f_{ads}(n)$, normalized for $n \geq 1$:

$$f_{ads}(n) = \sum_{j=1} p_j \frac{\lambda_j{}^n e^{-\lambda_j}}{n!(1 - e^{-\lambda_j})} \quad (2)$$

where the jth population of sites had a characteristic (i.e., mean) number of adsorption events, λ_j, and represented a fraction p_j of total sites, with $\sum p_j = 1$. The average site had $\lambda = \sum p_j\lambda_j$ adsorption events. With N total adsorption events, the number of predicted adsorption sites was given by N/λ. Therefore, the predicted adsorption site density takes into account the variation of adsorption sites strengths. By fitting the tail of the adsorption site distribution (i.e., for sites with $n \geq 1$), we were able to measure populations with less than one adsorption event on average. Simple counting of observed adsorption sites cannot accurately account for such populations of sites. For this reason, the number of predicted adsorption sites was a better indicator of the true surface site distribution than would be determined by simple site-counting.

On a perfectly homogeneous surface, proteins would adsorb to any surface site with equal probability. In order to evaluate the relative "heterogeneity" of a surface (i.e., the deviation from a perfectly adsorbing surface), we calculated a normalized heterogeneity parameter,

$$h = \frac{\text{maximum theoretical number of adsorption sites}}{\text{fitted number of adsorption sites}} = \frac{A/a}{N/\lambda}$$

where the imaged surface area was A and the molecule's footprint was a. As protein oligomers were rare, a values were specified as 5.6 nm^2 and 15.2 nm^2 for the area of BSA (ellipsoid) and IgG (y-shaped) monomers lying "side-on" with dimensions 4.0 × 4.0 × 14.0 nm^3 and 15.2 × 10.0 × 3.8 nm^3, respectively.[36,37] The relative heterogeneity measured for a surface also depended on the protein (e.g., BSA or IgG) used to probe the surface, since protein–surface interactions could depend on a protein's size, structure, or composition. For more heterogeneous surfaces, where the site adsorption events probability distribution was heavy-tailed, h was larger than for homogeneous surfaces. The error in h was calculated as the standard error between three or more experimental surface regions. The existence of discrete adsorption sites was independently confirmed by examining positional correlation between adsorption sites and is further discussed in the Supporting Information.

RESULTS AND DISCUSSION

It is frequently observed that membranes with nominally similar pore sizes and structures, but comprising different materials, exhibit different flux declines that are attributed to protein–material interactions.[15,16] The polymeric membrane surfaces considered here all showed similar static WCA (reflecting a surface's surface energy and hydrophobicity) and film thicknesses (see Table 1). To directly probe isolated protein–material (or in our case protein–surface) interactions, single-molecule interfacial dynamics were observed using sm-TIRFM at extremely dilute protein solution concentrations such that the average density of molecules on the surface was <0.1 molecule μm^{-2}. In addition, by adding higher concentrations of unlabeled protein (0.3–1.0 mg/mL), we were able to contrast interfacial protein behavior in the absence and presence of protein–protein interactions. Such conditions are

DOI: 10.1021/am507730k
ACS Appl. Mater. Interfaces 2015, 7, 3607–3617

relevant to the very initial and intermediate stages of protein adsorption to membrane interfaces, which may ultimately determine the structure of the adsorbed protein layer and the speed and extent of protein membrane fouling. Below we present (I) the role of protein population heterogeneity, (II) the role a surface spatial heterogeneity, and (III) the effects of increased protein concentrations on observed protein adsorption and desorption dynamics.

I. Protein Oligomers Remain on the Surface Longer than Protein Monomers. Each molecule in our experiments was characterized by its mean intensity, surface residence time, and molecular trajectory. Figure 1a shows a representative cumulative residence time distribution (CRTD) of IgG on RC. CRTDs were shown to be insensitive to photobleaching and photoblinking, see the Supporting Information, Figure S10. A single first-order desorption process would appear as a straight-line on the CRTD log−linear plot shown in Figure 1a. Instead, the curved CRTD can be modeled by a mixture of multiple first-order desorption processes (eq 1). As was the case for all surface and protein combinations examined, more than one characteristic residence time, or desorption rate, was required to fit these distributions, indicating heterogeneous protein dynamics. There are several potential sources for such heterogeneity including multiple oligomeric states at the surface: monomers, reversible (or irreversible) dimers, or even larger aggregate species (with different configurations and exposed hydrophobic and hydrophilic amino acid side groups). In addition, multiple protein conformations or orientations at the interface,[38] or surface regions or sites with different protein binding energies,[39] may also contribute to heterogeneous protein behavior. Initially, we considered the influence of oligomers (nonspecific dimers or larger oligomers formed in solution) on overall protein dynamics.

Kastantin et al. previously showed that protein monomers and oligomers (preformed in solution), were responsible for the heterogeneity observed in characteristic residence times for fibrinogen on various surfaces, including FS and TMS.[19] Because an object's mean fluorescence intensity indicates its oligomerization state (i.e., monomer, dimer, trimer, or larger oligomer), the authors used these fluorescence intensities to directly connect oligomerization state to populations identified by surface residence times (e.g., low intensity monomers accounted for the shortest-live characteristic residence time while oligomers accounted for longer characteristic residence times).

To evaluate the role of population heterogeneity (e.g., protein monomers, nonspecific dimers, trimers, and larger oligomers), we examined the mean fluorescence intensity distribution of all observed molecular trajectories. For each protein−surface combination, the distribution of fluorescence intensities was broad with a major peak at low intensity, as shown for IgG on RC in Figure 1b. At dilute protein concentrations, pH 7.4, and 25 °C, protein monomers represented the vast majority of molecules in solution. IgG and BSA solutions contained 96 ± 3% and 78 ± 3% monomers, respectively, as measured by size exclusion chromatography (see Figure S4 in the Supporting Information). Therefore, on the surface, we expect monomers to be represented by the major peak in the intensity distribution.[40] Indeed if we selected only molecules within this intensity peak and compared their desorption behavior to molecules selected from the high-intensity tail of the distribution, we found that the low intensity molecules were much shorter-lived, consistent with previous findings.[19] High-intensity objects (oligomers) were found to remain on the surface up to ten-times longer than low intensity objects (monomers), as shown in Figure 1c for IgG on RC. The mean characteristic residence times of monomers for all surface−protein combinations were 0.33−0.84 s while mean characteristic residence times of oligomers ranged from 0.99 ± 0.02 to 4.4 ± 0.9 s for IgG on PVAc-PVP/PES and FS, respectively, and from 1.7 ± 0.2 to 7 ± 1 s for BSA on the same respective surfaces (see Table S3 in Supporting Information).

At the protein surface coverage observed at such dilute protein concentrations (see Table S3 in Supporting Information), and considering that protein monomers remained on the surface for short times, we suspect that observed oligomers were most likely preformed in solution. If oligomers formed on the surface under these conditions, we might expect a molecule's fluorescence to increase, indicating oligomerizaiton. This does not appear to be the case; the probability distribution of all molecules' fluorescence intensities just after adsorption and just before desorption were similar (see Figure S11 in the Supporting Information).

Although less common, at any given time point, oligomers disproportionally accounted for more adsorbed species because they remained on the surface for much longer than monomers. We speculate that these oligomers would therefore be more likely to interact with other proteins on the surface and could nucleate further oligomerization and aggregation and, ultimately, protein layer formation. The consequence of aggregate surface adsorption was demonstrated by Kelly and Zydney where microfiltration membrane fouling and flux decline occurred much faster when large BSA aggregates were present in solution compared to aggregate-free solutions obtained after prefiltration.[10] They proposed a two-step process to explain this flux decline: (1) BSA aggregates deposit in early stages and (2) "native" (monomeric) BSA attach to deposited aggregates (nucleation sites) in later stages. Other researchers have reported similar phenomena for different membranes and proteins.[41,42] In a related study, Kelly et al. observed that raising just the ratio of BSA dimers to monomers led to a faster flux reduction in membrane filtration.[12] It is clear that population heterogeneity, and its kinetic consequences observed here, can contribute to macroscopically observed flux declines.

The residence time distributions were heavy-tailed, requiring two or three populations to fit monomer and oligomer residence time distributions (as per eq 1). This suggests there was significant heterogeneity in monomer-surface and oligomer-surface interactions. In the following section, we show that spatial variations are another important source of heterogeneity in interfacial dynamics.

II. Spatial Heterogeneity Increases Protein Residence Times. The unique capabilities of sm-TIRFM allowed us to spatially map heterogeneous protein dynamics on thin polymer films with high resolution (~50 nm). In general, spatial kinetic heterogeneity may be due to a combination of morphology/topography and surface chemistry. Kisley et al. used super-resolution imaging to identify and characterize protein adsorption to discrete charged sites on an agarose support involved in ion-exchange chromatography.[39,43] Similarly, Mabry et al. characterized strong adsorption sites on TMS functionalized silica and emphasized the importance of chemical surface heterogeneity.[22]

Although we expect commercial membranes to have morphological heterogeneity across many length scales, the thin polymer films studied here approximate some of the

DOI: 10.1021/am507730k
ACS Appl. Mater. Interfaces 2015, 7, 3607−3617

potential consequences of small-scale membrane surface spatial heterogeneity due to topographic (see AFM images in the Supporting Information) and possibly chemical heterogeneity. On the basis of the thickness and roughness of the polymer films (see Table 1 and Figure S3 in the Supporting Information), we are confident that the spin-coated polymer layers completely covered the underlying surface. We suggest that surface spatial heterogeneity observed on polymer films was most likely due to a combination of topography and surface chemistry. For example, cellulose can exist in several oxidation states and RC surfaces may have sites with several different oxidation states.[44] Our model hydrophilic and hydrophobic surfaces were also expected to exhibit spatial heterogeneity. On FS, we expect that silanol groups with hydrogen-bonding potential, may lead to favorable protein–surface interactions and strong binding sites. On TMS, we expect that some remaining uncapped silanol groups also will be present.[22]

Super-resolution maps of IgG and BSA adsorption events visually captured this spatial heterogeneity, as shown for IgG on RC in Figure 2a. Discrete sites where many protein adsorption events occurred could be clearly contrasted with sites where a single adsorption event occurred, over the course of the observation window. On a homogeneous surface, the probability of observing more than one adsorption event within a 50 nm site would be exceedingly low due to the finite number of adsorption events and so to observe such sites indicates anomalously strong binding. The super-resolution maps clearly revealed that all of the surfaces were heterogeneous and had anomalously strong sites (see Figure S6 in the Supporting Information). However, there was a wide distribution of protein–surface interaction strengths. Below we explore the consequences of this spatial heterogeneity.

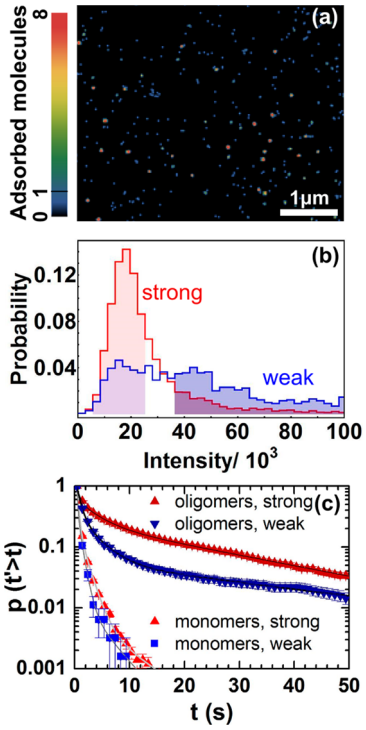

Figure 2. (a) Representative super-resolution map of 20 000 IgG adsorption events on RC. (b) Mean molecule fluorescence intensity probability distributions for IgG on RC at a dilute protein concentration. Molecules were separated by their initial location on either a strong ($n > 1$, red) or a weak site ($n = 1$, blue). (c) CRTDs for IgG on RC of monomers and oligomers initially adsorbed on either strong or weak sites. Multiple exponential fits to eq 1 are indicated by gray lines for each CRTD. The mean characteristic residence times of monomers and oligomers on strong or weak sites for all protein–surface combinations are tabulated in Table S2 in the Supporting Information.

a. Proteins Preferentially Adsorb to and Remain Longer on Anomalous "Strong" Surface Sites. We characterized the identities and dynamics of molecules adsorbing to anomalously strong and more prevalent weak binding sites. As mentioned above, an adsorption site where more than one adsorption event occurred was a highly unlikely occurrence because the number of potential surface adsorption sites was much greater than the number of molecules observed in our single-molecule experiments. For example, for the super-resolution map shown in Figure 2a, we observed 20 000 IgG adsorption events on a RC surface image area of 0.011 mm^2. Given that an IgG monomer occupies an area of 1.2×10^{-10} mm^2, the observed molecules covered less than 0.02% of the total surface area imaged. Therefore, we nominally classified anomalous "strong" sites as sites with more than one adsorption event ($n > 1$, where n is the number of adsorption events) and "weak" sites as sites where only one adsorption event occurred ($n = 1$). Similar strong sites (or adsorption hot spots) have been observed on TMS previously.[22]

For all protein–surface combinations, monomers were much more likely to be observed on the strong sites than on weak sites, despite the presumed prevalence of weak sites. This can be seen in Figure 2b, where the monomer intensity peak dominates the strong adsorption site intensity distribution for IgG on RC. In contrast, IgG objects observed on weak sites were equally likely to be monomers, dimers, and larger oligomers. It is tempting to interpret this observation as suggesting that monomers preferentially adsorb to strong sites. However, due to the finite acquisition time (0.2 s) used in our experiments, it is more likely that monomers also adsorbed on weak sites but resided on these sites for very short periods of time such that they were not observed. This appeared to be the case when we examined monomer residence times on weak and strong sites. The mean characteristic residence times of IgG monomers on weak sites were between 0.2 and 0.4 s whereas the characteristic residence times of IgG monomers on strong sites were nearly twice as long (0.5–0.8 s) on the polymer films (see the Supporting Information, Table S2). Despite only observing the relatively "long-lived" tail of monomers on weak sites, by fitting the entire residence time distribution we could infer the behavior of the "short-lived" monomers as well.[34,45] The mean characteristic residence times indicated that we observed fewer monomers adsorbing on weak sites compared with strong sites.

In fact, both monomers and oligomers were found to reside on strong sites longer than on weak sites as shown in Figure 2c for IgG on RC (see the Supporting Information for mean characteristic times for all protein–surface combinations). From this finding, and the observation of more adsorption events on strong sites, we can infer that protein–surface interactions on strong sites were associated with greater adsorption free energies than on weaker sites. This also suggests, that, while less common, strong sites disproportionally adsorb proteins. We propose that proteins remaining longer on these strong sites have more opportunities to reorient, undergo conformation changes, and interact with other proteins. Therefore, surfaces with more anomalous sites and/or sites

DOI: 10.1021/am507730k
ACS Appl. Mater. Interfaces 2015, 7, 3607–3617

with stronger protein−surface binding could develop a protein layer faster.

b. Surfaces Exhibit a Distribution of Surface Sites. To quantify a given surface's relative spatial heterogeneity, we examined the distribution of adsorption event counts per surface site. Figure 3 shows three representative probability

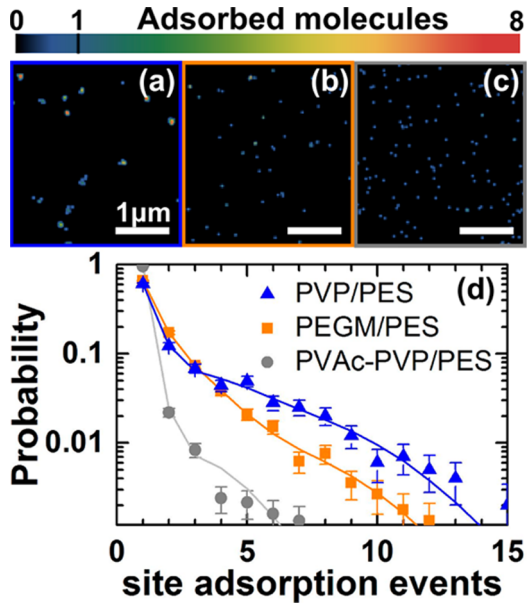

Figure 3. Representative super-resolution maps of 5000 IgG adsorption events on (a) PVP/PES, (b) PEGM/PES, and (c) PVAc-PVP/PES. (d) Probability distribution of IgG site adsorption event counts for sites identified on PVP/PES, PEGM/PES, and PVAc-PVP/PES for 5000 IgG adsorption events on each surface.

histograms of site adsorption event counts for IgG on PVP/PES, PEGM/PES, and PVAc-PVP/PES (the adsorption event probability distribution on RC was similar to those of PEGM/PES and PVP/PES). The adsorption event count histograms shown in Figure 3 were created from 5000 adsorption events on surface areas of 0.01 mm^2. If surfaces were homogeneous, where every surface site had the same adsorption probability, we would expect these distributions to follow a single Poisson distribution. It is clear, however, that these distributions are heavy-tailed, with some sites adsorbing proteins much more frequently than others. This suggests that these surfaces were not homogeneous, since a single Poisson distribution did not adequately explain the data. Instead, we assumed that adsorption resulted from multiple types of sites exhibiting first-order kinetics and fit each histogram with a multicomponent Poisson distribution (eq 2). This assumption is consistent with previous studies that have shown individual sites exhibit first-order kinetics.[39]

With a finite number of trajectories, we observed adsorption on only a fraction of the potential sites. However, for a given site, the number of adsorption events followed a Poisson distribution, and we could fit the tail of this distribution (i.e., when $n \geq 1$) to estimate the density of adsorption sites, which was related to the surface heterogeneity, h. We note that our 200 ms time resolution limited our ability to observe molecules on weak sites with characteristic residence times shorter than our acquisition time, and so our estimated site density would be expected to have a dependence on acquisition time. However, when we compared the site adsorption event count distributions of 1000 BSA trajectories on FS at an acquisition times of either 100 or 200 ms, we saw no significant changes over this factor of 2 difference (see Figure S13 in the Supporting Information). Ultimately, we imaged all of our surfaces under similar conditions (i.e., acquisition time of 200 ms) such that we could consistently compare the heterogeneity of the different surfaces.

With these considerations in mind, we compared adsorption event histograms across surfaces in both qualitative and semiquantitative ways. As shown in Figure 3, the site adsorption event histograms varied widely between surfaces. For example, PVP/PES and PEGM/PES site adsorption event distributions were more completely explained by three types of sites (i.e., three Poisson distributions) whereas, for PVAc-PVP/PES, two types of sites sufficed to describe the narrower distribution, suggesting that PVAc-PVP/PES surfaces were more homogeneous. Further, based on the multicomponent Poisson distribution fitting, the majority of sites (97, 67, and 66%) were weak sites, with characteristic adsorption event counts of 0.036 ± 0.008, 0.30 ± 0.04, and 0.26 ± 0.05 for PVAc-PVP/PES, PEGM/PES, and PVP/PES, respectively. All three surfaces had a second population of stronger sites with characteristic adsorption event counts of 3.0 ± 0.6, 2.2 ± 0.3,

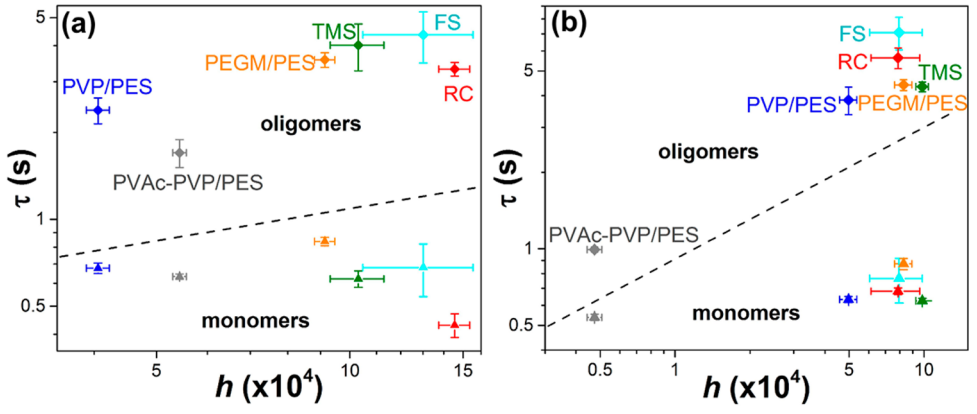

Figure 4. Relationship between heterogeneity, h, and protein monomer and oligomer mean characteristic residence times on FS (cyan), RC (red), TMS (green), PEGM/PES (orange), PVP/PES (blue), and PVAc-PVP/PES (gray) for (a) BSA and (b) IgG. N was set at 1000 trajectories for all protein−surface combinations. Error bars represent the standard error between experimental surface regions. Mean characteristic residence times for monomers and oligomers for all surface−protein combinations are tabulated in Table S3 of the Supporting Information.

DOI: 10.1021/am507730k
ACS Appl. Mater. Interfaces 2015, 7, 3607−3617

and 3.3 ± 0.6, representing 3, 28, and 23% of sites for PVAc-PVP/PES, PEGM/PES, and PVP/PES respectively. PEGM/PES and PVP/PES had an additional rare population of strong-binding sites representing 5 and 11% of sites with characteristic adsorption event counts of 6.6 ± 0.7 and 7 ± 1, respectively. A PVAc-PVP/PES surface not only had fewer types of adsorption sites but was also comprised mainly of sites with weaker adsorption than was observed on PVP/PES and PEGM/PES. Based upon this analysis, we could conclude that PVAc-PVP/PES surfaces were more homogeneous than PVP/PES and PEGM/PES.

c. More Homogeneous Surfaces Are Correlated with Shorter-Lived Adsorbed Proteins. As discussed above, site adsorption event histograms reflected a surface's spatial heterogeneity. In order to compare the relative spatial heterogeneity between different surface chemistries we calculated a dimensionless "heterogeneity" parameter, h, for each surface as defined in the Materials and Methods section. Surfaces with low h values were more homogeneous than surfaces with high h values. Figure 4 shows the intriguing relationship between the mean characteristic residence times of monomers and oligomers and the surface heterogeneity, h. Monomer mean residence times were short-lived (~0.7 s) and similar for both proteins on all surfaces, suggesting that any actual variation in residence time was likely well below our time resolution. For oligomers, the mean characteristic residence times increased systematically with increasing h. This suggests that increasing surface homogeneity (by reducing the density and strength of strong adsorption sites) led to shorter residence times and that this surface heterogeneity metric may be a good predictor of oligomer residence times and ultimately membrane surface fouling.

This relationship was most pronounced for PVAc-PVP/PES and FS surfaces that represented extremely homogeneous and extremely heterogeneous behavior, respectively. The oligomer surface residence times of BSA and IgG on PVAc-PVP/PES were, on average, two and four times shorter, respectively, than on all other surfaces (see Supporting Information, Table S3). Because protein−surface interactions were most homogeneous and weakest on PVAc-PVP/PES compared with other wetting agents added to PES, this suggests that PVAc-PVP may also reduce protein membrane fouling better than the other wetting agents considered here.

IgG oligomer residence times varied more than BSA residence times on surfaces with similar homogeneity. For example, IgG oligomers resided longer on hydrophilic FS surfaces than on more hydrophobic TMS and PEGM/PES. This suggests that IgG interfacial dynamics were more sensitive to surface chemistry than were BSA interfacial dynamics. Such differences are not particularly surprising since BSA and IgG differ in several characteristics including the structure and the reversibility and intermolecular forces involved in oligomerization and aggregation. For example, BSA oligomers have been shown to be stabilized by intermolecular disulfide bonds.[46]

Despite hydrophobicity differences between hydrophilic FS and hydrophobic TMS, we observed similar residence times for both oligomers and monomers on both surfaces at dilute protein concentrations. This was consistent with previous single-molecule findings where both fibrinogen and BSA residence times were similar on FS and TMS surfaces.[19,47] Therefore, desorption kinetics of isolated proteins depend on molecular phenomena that appear to be uncorrelated with macroscopic hydrophobicity.

III. Increased Protein Concentrations Leads to Reduced Protein Surface Residence Times and Increased Surface Homogeneity. We have shown that at extremely dilute protein concentrations anomalous strong adsorption sites disproportionally account for proteins adsorbed to the surface and that proteins reside on these sites for significantly longer times, which may contribute to surface fouling. However, real membrane separations typically occur at high protein concentrations where protein−protein interactions could become more significant than protein−surface interactions. In previous work, we demonstrated that dynamic protein−protein interfacial associations occurred at solution concentrations as low as 2.5×10^{-6} mg/mL for BSA on a PEG monolayer (at a surface coverage of 2.5 molecules per μm^2).[45]

In the experiments described in this section, protein solution concentrations were increased to 0.3 mg/mL for IgG and 1.0 mg/mL for BSA by mixing unlabeled protein and low concentrations of fluorescently labeled protein (10^{-5}−10^{-6} mg/mL). Labeled proteins served as reporter molecules of interfacial dynamics at these high protein concentrations. Experiments at dilute (labeled protein only) and high (labeled and unlabeled protein) concentrations were performed sequentially on the same surface sample, and therefore any resulting differences in dynamics were due primarily to increased surface coverage. The same solution concentration for each protein was used for all surfaces to account for the fact that protein surface coverage may vary on different surface chemistries. The surface coverage at high concentrations, for all protein−surface combinations, was at minimum 4 orders of magnitude greater than in the extremely dilute case described earlier. Calculated values for the fractional surface coverage are reported in the Supporting Information (Table S3). In brief, the surface coverage varied from less than one percent of monolayer coverage (BSA on PVAc-PVP/PES and PVP/PES) to full monolayer coverage (IgG on TMS and PVP/PES). In comparing the surfaces, we found that surface heterogeneity was positively correlated with higher protein surface coverage (Table S3). This finding was consistent with our hypothesis that more heterogeneous surfaces accelerate protein layer formation.

At high protein concentrations, anomalous strong sites, which had been apparent at dilute concentrations, possibly were occupied by adsorbed proteins, preventing further adsorption to these sites. We term this phenomenon "site blocking". As shown in Figure 5a and b for IgG on PVP/PES, the relatively strong sites that were identified at high protein concentrations had fewer adsorption events than on the same surface in contact with very dilute protein concentrations. The surface map at a very dilute concentration in Figure 5a has many strong sites and few weak sites while the surface map at high protein concentration in Figure 5b has more weak sites and relatively few strong sites. These qualitative observations were quantified in the site adsorption events probability distribution for 10 000 IgG adsorption events on PVP/PES (Figure 5c) for both protein concentration conditions. The fraction of strong sites was reduced (6 ± 1%) at a high protein concentration compared to that measured at dilute protein concentration conditions (32 ± 3%).

In addition, IgG surface residence times at high protein concentrations were shorter than at extremely dilute concentrations on PVP/PES surfaces as shown in Figure 6, potentially as a result of adsorbed protein blocking further adsorption on

DOI: 10.1021/am507730k
ACS Appl. Mater. Interfaces 2015, 7, 3607−3617

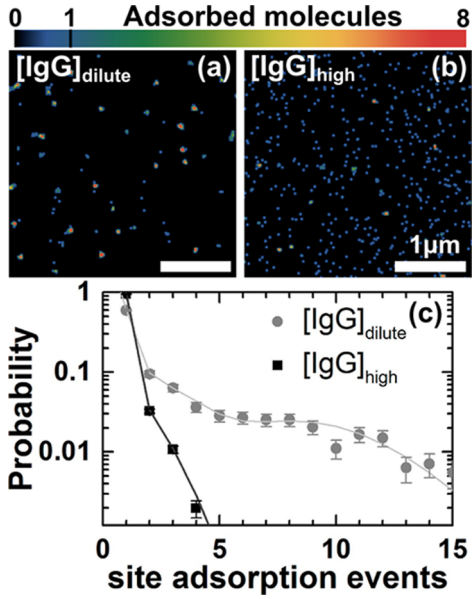

Figure 5. Super-resolution maps of 10 000 IgG adsorption events on PVP/PES (a) at an extremely dilute (10^{-6} mg/mL) and (b) high (0.3 mg/mL) IgG concentration. (c) Site adsorption event probability distributions for 10 000 IgG adsorption events on PVP/PES at 10^{-6} mg/mL (gray) and 0.3 mg/mL (black) IgG concentrations.

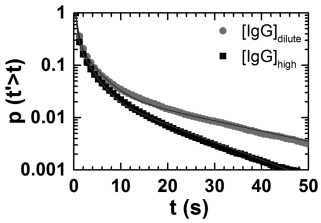

Figure 6. CRTDs for all IgG molecules (monomers and oligomers) on PVP/PES for an extremely dilute protein concentration (10^{-6} mg/mL, gray circles) and a high protein concentration (0.3 mg/mL, black squares). The multiple exponential population fit parameters to eq 1 are tabulated in Table S4 in the Supporting Information.

strong sites, as suggested above. If the surfaces were perfectly homogeneous, we would expect the opposite trend, since protein−protein associations would result in more oligomers at the interface, which have longer residence times. For example, in previous work, transient protein−protein associations were observed to increase the surface residence time for BSA on a PEG monolayer at protein concentrations as low as 2.5×10^{-6} mg/mL.[45] Although molecular fluorescence intensity serves as only a lower estimate of oligomerization state when unlabeled proteins are present, we saw both fluorescently labeled monomers and oligomers at high protein concentrations on the surface (see the Supporting Information). For both monomers and oligomers, we observed shorter residence times at high protein concentrations. This suggests that surface heterogeneity had a greater impact on residence times than lateral protein−protein associations at high protein concentrations.

This phenomenon of increased homogeneity and decreased residence times at high protein concentration was observed for all but the most homogeneous surfaces (Table S3, Supporting Information). Of the 12 protein−surface combinations, at high protein concentrations, 9 showed an increase in homogeneity by an average factor of 2 (with the exception of BSA on PVP/PES and IgG on PVAc-PVP/PES and FS), and 10 showed decreased residence time by an average factor of 2 (with the exception of IgG on PVAc-PVP/PES and RC). On none of the surfaces did we see a significant increase in residence times as protein concentration was increased (Table S3, Supporting Information).

By comparing dilute and high protein concentrations, we were able to demonstrate interesting contrasts between surface chemistries. In particular, protein surface dynamics on PVAc-PVP/PES and PEGM/PES were markedly different. Both are promising protein-resistant surfaces when strong sites are greatly reduced (in the case of PVAc-PVP/PES) or blocked (in the case of PEGM/PES). PVAc-PVP/PES was the most homogeneous surface, with fewer and weaker anomalous sites and short residence times at both dilute and high protein concentrations, as discussed above. In contrast, PEGM/PES was much more heterogeneous, and the residence time decrease from dilute to high protein concentrations was the most dramatic decrease of all surfaces. On PEGM/PES the average characteristic residence times of all molecules at dilute and high IgG concentrations were 1.8 ± 0.1 and 0.33 ± 0.02 s respectively, almost an order of magnitude different (Table S3 in the Supporting Information). This suggests that the effect of blocking strong sites can be quite pronounced for more heterogeneous surfaces.

Another possible explanation for the reduced surface residence times at high protein concentrations is that protein−protein interactions may lead to reduced protein affinity for the surface. Unfavorable protein−protein interactions (e.g., due to electrostatics, confinement, etc.) in the adsorbed state have been previously proposed in the literature.[48,49] However, our previous work with BSA showed that protein−protein associations led to increased surface affinity, and we hypothesized that BSA and IgG self-association was likely to increase surface affinity here as well.[45] Thus, we conclude that site blocking, and not protein−protein interactions, likely played a dominant role in the apparent decrease of protein surface affinity at high concentrations.

Surface exchange (i.e., the displacement of adsorbed proteins from the surface by proteins in solution) may also play a role in reducing surface residence times at high protein concentrations, where orders of magnitude more proteins were in solution.[50] However, we would not predict the striking change in the distribution of strong and weak surface sites nor the correlation between residence time and surface heterogeneity if surface exchange were the sole mechanism at play at high concentration. Instead, although surface exchange may play a role in reducing residence times, site blocking appeared to be the dominant cause of both reduced residence times and heterogeneity.

CONCLUSIONS

By observing individual BSA and IgG surface dynamics on polymer films with sm-TIRFM, population and spatial heterogeneity were both shown to influence protein desorption. At extremely dilute protein concentrations, protein oligomers, though less common, remained up to 10 times longer on surfaces than protein monomers. Proteins, both monomers and oligomers, also remained longer on more heterogeneous surfaces that contained anomalously strong surface sites. More proteins adsorbed and resided up to two times longer on strong sites than on more prevalent weak surface sites. We propose two potential mechanistic consequences of population

DOI: 10.1021/am507730k
ACS Appl. Mater. Interfaces 2015, 7, 3607−3617

and spatial heterogeneity relevant to membrane fouling: (1) longer-lived protein oligomers have more opportunities to interact with other surface species and therefore can nucleate further oligomerization and aggregation, accelerating protein layer formation; (2) anomalously strong sites effectively collect more protein monomers and oligomers and thus facilitate protein−protein associations, potentially leading to oligomerization and accelerated protein layer formation.

At high protein concentrations, we observed a decrease in both spatial heterogeneity and residence times for the majority of protein−surface combinations. We propose that at higher concentrations, adsorbed proteins block further protein adsorption on strong sites. This suggests that at higher surface coverage heterogeneity can be mitigated by adsorbed proteins in the near surface environment.

From these findings, we recommend reducing population heterogeneity (e.g., by prefiltering protein solutions if possible) and spatial heterogeneity (e.g., reducing the presence of anomalous sites by creating more topographically and chemically homogeneous membranes or by adding blocking agents to solutions) in order to reduce protein membrane fouling. We have demonstrated a comprehensive method of characterizing and quantifying these anomalous sites. The PVAc-PVP/PES polymer blend films appeared to reduce protein residence times, and to be the most homogeneous surfaces at both dilute and high protein concentrations.

The differences observed between BSA and IgG interfacial behavior also highlight the importance of protein properties when studying membrane fouling. Often protein membrane fouling on novel membrane materials is characterized with only one type of protein feed solution, frequently BSA. As demonstrated here, BSA fouling behavior may not be representative of all protein fouling.

Finally, we note that protein oligomers and strong sites are rare phenomena, not necessarily captured with ensemble-averaged measurements. Thus, single-molecule methods are uniquely suited for studying such phenomena.

■ ASSOCIATED CONTENT

Ⓢ Supporting Information

Polymer film preparation, topographic surface characterization, protein solution characterization, population heterogeneity at dilute protein concentrations, strong vs weak site desorption kinetics, surface heterogeneity and protein desorption kinetics, population heterogeneity at high protein concentrations, adsorption event position correlation analysis, power studies showing no photophysical effects, adsorption and desorption fluorescence intensity histograms, residence time and site adsorption distributions showing no dependence on tracking radius, and site adsorption distributions showing no dependence on acquisition time. This material is available free of charge via the Internet at http://pubs.acs.org.

■ AUTHOR INFORMATION

Corresponding Author

*D. K. Schwartz. E-mail: daniel.schwartz@colorado.edu.

Notes

The authors declare no competing financial interest.

■ ACKNOWLEDGMENTS

The authors (B.B.L., R.B.M., and I.S.) acknowledge primary support from Pall Corp. for many aspects of the research reported here, including salary and stipend support and polymer materials. Support for the development of high-throughput dual-channel tracking methods and instrumentation was provided by the U.S. Department of Energy Basic Energy Sciences, Chemical Sciences, Geosciences, and Biosciences Division (No. DE-SC0001854). J.N.M. was partially supported by a U.S. Department of Education Graduate Assistance in Areas of National Need Fellowship (No. P200A120125). O.J.R. is grateful for funding support by the Academy of Finland through its Center of Excellence Program (2014-2019) "Molecular Engineering of Biosynthetic Hybrid Materials Research" (HYBER). We also thank Professor Ted Randolph and Lea Sorret at the University of Colorado Boulder for access to and assistance with their high performance liquid chromatography system.

■ REFERENCES

(1) van Reis, R.; Zydney, A. Bioprocess Membrane Technology. *J. Membr. Sci.* **2007**, *297*, 16−50.
(2) Zydney, A. L. Membrane Technology for Purification of Therapeutic Proteins. *Biotechnol. Bioeng.* **2009**, *103*, 227−230.
(3) Saxena, A.; Tripathi, B. P.; Kumar, M.; Shahi, V. K. Membrane-based Techniques for the Separation and Purification of Proteins: An Overview. *Adv. Colloid Interface Sci.* **2009**, *145*, 1−22.
(4) Charcosset, C. Membrane Processes in Biotechnology: An Overview. *Biotechnol. Adv.* **2006**, *24*, 482−492.
(5) Nabe, A.; Staude, E.; Belfort, G. Surface Modification of Polysulfone Ultrafiltration Membranes and Fouling by BSA Solutions. *J. Membr. Sci.* **1997**, *133*, 57−72.
(6) Chan, R.; Chen, V. Characterization of Protein Fouling on Membranes: Opportunities and Challenges. *J. Membr. Sci.* **2004**, *242*, 169−188.
(7) Zydney, A. L. Nonspecific Protein-Membrane Interactions: Adsorption and Fouling. In *Biofunctional Membranes*; Butterfield, D. A., Ed.; Plenum Press: New York, 1996; pp 279−288.
(8) Kastantin, M.; Langdon, B. B.; Schwartz, D. K. A Bottom-up Approach to Understanding Protein Layer Formation at Solid-Liquid Interfaces. *Adv. Colloid Interface Sci.* **2014**, *207*, 240−252.
(9) Bowen, W. R.; Calvo, J. I.; Hernández, A. Steps of Membrane Blocking in Flux Decline during Protein Microfiltration. *J. Membr. Sci.* **1995**, *101*, 153−165.
(10) Reihanian, H.; Robertson, C. R.; Michaels, A. S. Mechanisms of Polarization and Fouling of Ultrafiltration Membranes by Proteins. *J. Membr. Sci.* **1983**, *16*, 237−258.
(11) Kelly, S. T.; Zydney, A. L. Mechanisms for BSA Fouling during Microfiltration. *J. Membr. Sci.* **1995**, *107*, 115−127.
(12) Kelly, S. T.; Opong, W. S.; Zydney, A. L. The Influence of Protein Aggregates on the Fouling of Microfiltration Membranes during Stirred Cell Filtration. *J. Membr. Sci.* **1993**, *80*, 175−187.
(13) Oom, A.; Poggi, M.; Wikström, J.; Sukumar, M. Surface Interactions of Monoclonal Antibodies Characterized by Quartz Crystal Microbalance with Dissipation: Impact of Hydrophobicity and Protein Self-interactions. *J. Pharm. Sci.* **2011**, *101*, 519−529.
(14) Liu, S. X.; Kim, J. T. Application of Kevin−Voigt Model in Quantifying Whey Protein Adsorption on Polyethersulfone Using QCM-D. *JALA* **2009**, *14*, 213−220.
(15) Huisman, I. H.; Prádanos, P.; Hernández, A. The Effect of Protein−Protein and Protein−Membrane Interactions on Membrane Fouling in Ultrafiltration. *J. Membr. Sci.* **2000**, *179*, 79−90.
(16) Pieracci, J.; Crivello, J. V.; Belfort, G. Photochemical Modification of 10 kDa Polyethersulfone Ultrafiltration Membranes for Reduction of Biofouling. *J. Membr. Sci.* **1999**, *156*, 223−240.
(17) Kastantin, M.; Walder, R.; Schwartz, D. K. Identifying Mechanisms of Interfacial Dynamics Using Single-Molecule Tracking. *Langmuir* **2012**, *28*, 12443−12456.

DOI: 10.1021/am507730k
ACS Appl. Mater. Interfaces 2015, 7, 3607−3617

(18) Walder, R.; Kastantin, M.; Schwartz, D. K. High Throughput Single Molecule Tracking for Analysis of Rare Populations and Events. *Analyst* **2012**, *137*, 2987−2996.
(19) Kastantin, M.; Langdon, B. B.; Chang, E. L.; Schwartz, D. K. Single-Molecule Resolution of Interfacial Fibrinogen Behavior: Effects of Oligomer Populations and Surface Chemistry. *J. Am. Chem. Soc.* **2011**, *133*, 4975−4983.
(20) Walder, R.; Schwartz, D. K. Single Molecule Observations of Multiple Protein Populations at the Oil-Water Interface. *Langmuir* **2010**, *26*, 13364−13367.
(21) Walder, R.; Nelson, N.; Schwartz, D. K. Super-Resolution Surface Mapping Using the Trajectories of Molecular Probes. *Nat. Commun.* **2011**, *2*, 515.
(22) Mabry, J. N.; Skaug, M. J.; Schwartz, D. K. Single-Molecule Insights into Retention at a Reversed-Phase Chromatographic Interface. *Anal. Chem.* **2014**, *86*, 9451−9458.
(23) Sethuraman, A.; Han, M.; Kane, R. S.; Belfort, G. Effect of Surface Wettability on the Adhesion of Proteins. *Langmuir* **2004**, *20*, 7779−7788.
(24) Mahendran, R.; Malaisamy, R.; Mohan, D. R. Cellulose Acetate and Polyethersulfone Blend Ultrafiltration Membranes. Part I: Preparation and Characterizations. *Polym. Adv. Technol.* **2004**, *15*, 149−157.
(25) Zhao, C.; Xue, J.; Ran, F.; Sun, S. Modification of Polyethersulfone Membranes − A Review of Methods. *Prog. Mater. Sci.* **2013**, *58*, 76−150.
(26) Susanto, H.; Ulbricht, M. Characteristics, Performance and Stability of Polyethersulfone Ultrafiltration Membranes Prepared by Phase Separation Method Using Different Macromolecular Additives. *J. Membr. Sci.* **2009**, *327*, 125−135.
(27) Weis, A.; Bird, M. R.; Nyström, M.; Wright, C. The Influence of Morphology, Hydrophobicity and Charge upon the Long-Term Performance of Ultrafiltration Membranes Fouled with Spent Sulphite Liquor. *Desalination* **2005**, *175*, 73−85.
(28) Kontturi, E.; Thüne, P. C.; Niemantsverdriet, J. W. Cellulose Model Surfaces - Simplified Preparation by Spin Coating and Characterization by X-ray Photoelectron Spectroscopy, Infrared Spectroscopy, and Atomic Force Microscopy. *Langmuir* **2003**, *19*, 5735−5741.
(29) Schaub, M.; Wenz, G.; Wegner, G.; Stein, A.; Klemm, D. Ultrathin Films of Cellulose on Silicon Wafers. *Adv. Mater.* **1993**, *5*, 919−922.
(30) Holmberg, M.; Berg, J.; Stemme, S.; Ödberg, L.; Rasmusson, J.; Claesson, P. Surface Force Studies of Langmuir-Blodgett Cellulose Films. *J. Colloid Interface Sci.* **1997**, *186*, 369−381.
(31) Kontturi, E.; Suchy, M.; Penttilä, P.; Jean, B.; Pirkkalainen, K.; Torkkeli, M.; Serimaa, R. Amorphous Characteristics of an Ultrathin Cellulose Film. *Biomacromolecules* **2011**, *12*, 770−777.
(32) Köhler, S.; Liebert, T.; Heinze, T. Interactions of Ionic Liquids with Polysaccharides. VI. Pure Cellulose Nanoparticles from Trimethylsilyl Cellulose Synthesized in Ionic Liquids. *J. Polym. Sci., Part A: Polym. Chem.* **2008**, *46*, 4070−4080.
(33) Norde, W.; Favier, J. P. Structure of Adsorbed and Desorbed Proteins. *Colloids Surf.* **1992**, *64*, 87−93.
(34) Kastantin, M.; Schwartz, D. K. Identifying Multiple Populations from Single-Molecule Lifetime Distributions. *ChemPhysChem* **2013**, *14*, 374−380.
(35) Chen, J. X.; Bremauntz, A.; Kisley, L.; Shuang, B.; Landes, C. F. Super-Resolution mbPAINT for Optical Localization of Single-Stranded DNA. *ACS Appl. Mater. Interfaces* **2013**, *5*, 9338−9343.
(36) Buijs, J.; Lichtenbelt, J. W. T.; Norde, W.; Lyklema, J. Adsorption of Monoclonal IgGs and Their $F(ab')_2$ Fragments onto Polymeric Surfaces. *Colloids Surf., B* **1995**, *5*, 11−23.
(37) Wertz, C. F.; Santore, M. M. Adsorption and Relaxation Kinetics of Albumin and Fibrinogen on Hydrophobic Surfaces: Single-Species and Competitive Behavior. *Langmuir* **1999**, *15*, 8884−8894.
(38) McLoughlin, S. Y.; Kastantin, M.; Schwartz, D. K.; Kaar, J. L. Single-Molecule Resolution of Protein Structure and Interfacial Dynamics on Biomaterial Surfaces. *Proc. Natl. Acad. Sci. U. S. A.* **2013**, *110*, 19396−19401.
(39) Kisley, L.; Chen, J.; Mansur, A. P.; Shuang, B.; Kourentzi, K.; Poongavanam, M. V.; Chen, W. H.; Dhamane, S.; Willson, R. C.; Landes, C. F. Unified Superresolution Experiments and Stochastic Theory Provide Mechanistic Insight into Protein Ion-Exchange Adsorptive Separations. *Proc. Natl. Acad. Sci. U. S. A.* **2014**, *111*, 2075−2080.
(40) Babcock, J. J.; Brancaleon, L. Bovine Serum Albumin Oligomers in the E- and B-Forms at Low Protein Concentration and Ionic Strength. *Int. J. Biol. Macromol.* **2013**, *53*, 42−53.
(41) Kanani, D. M.; Sun, X.; Ghosh, R. Reversible and Irreversible Membrane Fouling during in-Line Microfiltration of Concentrated Protein Solutions. *J. Membr. Sci.* **2008**, *315*, 1−10.
(42) Cutler, H. E.; Husson, S. M.; Wickramasinghe, S. R. Prefiltration to Suppress Protein Fouling of Microfiltration Membranes. *Sep. Purif. Technol.* **2012**, *89*, 329−336.
(43) Kisley, L.; Chen, J.; Mansur, A. P.; Dominguez-Medina, S.; Kulla, E.; Kang, M. K.; Shuang, B.; Kourentzi, K.; Poongavanam, M. V.; Dhamane, S.; Willson, R. C.; Landes, C. F. High Ionic Strength Narrows the Population of Sites Participating in Protein Ion-Exchange Adsorption: A Single-Molecule Study. *J. Chromatogr. A* **2014**, *1343*, 135−142.
(44) Rutherford, H. A.; Minor, F. W.; Martin, A. R.; Harris, M. Oxidation of Cellulose: The Reaction of Cellulose with Periodic Acid. *J. Res. Natl. Bur. Stand. (U. S.)* **1942**, *29*, 131−141.
(45) Langdon, B. B.; Kastantin, M.; Walder, R.; Schwartz, D. K. Interfacial Protein-Protein Associations. *Biomacromolecules* **2014**, *15*, 66−74.
(46) Maruyama, T.; Katoh, S.; Nakajima, M.; Nabetani, H. Mechanism of Bovine Serum Albumin Aggregation during Ultrafiltration. *Biotechnol. Bioeng.* **2001**, *75*, 233−238.
(47) Langdon, B. B.; Kastantin, M.; Schwartz, D. K. Apparent Activation Energies Associated with Protein Dynamics on Hydrophobic and Hydrophilic Surfaces. *Biophys. J.* **2012**, *102*, 2625−2633.
(48) Sethuraman, A.; Belfort, G. Protein Structural Perturbation and Aggregation on Homogeneous Surfaces. *Biophys. J.* **2005**, *88*, 1322−1333.
(49) Rabe, M.; Verdes, D.; Rankl, M.; Artus, G. R. J.; Seeger, S. A Comprehensive Study of Concepts and Phenomena of the Nonspecific Adsorption of Beta-Lactoglobulin. *ChemPhysChem* **2007**, *8*, 862−872.
(50) Vogler, E. A. Protein Adsorption in Three Dimensions. *Biomaterials* **2012**, *33*, 1201−1237.

DOI: 10.1021/am507730k
ACS Appl. Mater. Interfaces 2015, 7, 3607−3617